Microstimulation of the Lumbosacral Spinal Cord: Mapping

NIH-NINDS-NO1-NS-8-2300

Quarterly Progress Report #1

Period Covered: 30 September, 1998 - 31 December, 1998

Principal Investigator: Warren M. Grill, Ph.D.

Co-Investigators: Musa A. Haxiu, M.D., Ph.D.
                    Michel A. Lemay, Ph.D.

Department of Biomedical Engineering
Case Western Reserve University
Cleveland, OH 44106-4912

ABSTRACT

The objectives of this research are to determine the anatomical locations of spinal neurons involved in control of the genitourinary and hindlimb motor systems, and to determine the physiological responses evoked in the genitourinary and hindlimb motor systems by intraspinal microstimulation. During this quarter we made progress toward both of these objectives. We used double immunocytochemistry to identify spinal neurons that express c-Fos and GABA after isometric micturition. The results indicate that less than five percent of spinal neurons active during reflex micturition exhibit GABAergic traits, and are consistent with our previous work co-localizing c-Fos with parvalbumin. We began a series of experiments to characterize the hindlimb motor responses evoked by microstimulation of the lumbar spinal cord. The results demonstrate that endpoint forces provide a more complete characterization of the hindlimb motor response evoked by microstimulation than single joint torques. Microstimulation in intermediate regions produced endpoint force patterns that converged to a point in the limb workspace, while microstimulation in the ventral region produced parallel or divergent patterns of forces at the endpoint.

INTRODUCTION

Electrical stimulation of the nervous system is a means to restore function to individuals with neurological disorders. The objective of this project is to investigate the feasibility of neural prosthetics based on microstimulation of the spinal cord with penetrating electrodes. Specifically, chemical and viral retrograde tracers, immediate early gene expression, and immunocytochemistry are used to determine the locations and neurochemical content of neurons in the spinal cord that control genitourinary and motor functions in the male cat. Microstimulation with penetrating activated iridium microelectrodes to determine the physiological effects in the genitourinary and motor systems of activation of different neural populations. The results of this project will provide data important to understanding neural control of genitourinary and motor functions, answer fundamental questions about microstimulation of the spinal cord, and lead to development of a new generation of neural prosthetics for individuals with neurological impairments.

PROGRESS IN THIS QUARTER

During the first quarter of this contract we conducted a series of experiments to determine the location of neurons active during reflex micturition that contain gamma-amino butyric acid (GABA), and are thus likely serve an inhibitory function. We also began a series of experiments to measure the endpoint force produced at the hindlimb by microstimulation of the lumbar spinal cord. These studies will extend our previous single

joint mapping studies to consider the behavior of the whole limb. Below each of our accomplishments is summarized.

Identification of Neurons Involved in Control of Micturition

During relfex micturition the motoneurons innervating the external urethral sphincter are synaptically inhibited and pudendal afferent fibers receive presynaptic inhibition. The objective of these experiments is to identify inhibitory neurons that are active during reflex micturition. Co-localization of c-Fos, the protien product of the immediate early gene c-fos, and the neurotransmitter gamma-amino butyric acid (GABA) was used to identify putative inhibitory neurons that are active during reflex micturition. We have previously used patterns of c-Fos expression to identify spinal neurons active during reflex micturition in the male cat [Grill et al., 1998a]. The present results demonstrate that less than 5% of neurons immunoreactive for c-Fos (i.e., active during reflex micturition) are also immunoreactive for GABA, a finding consistent with our previous studies employing co-localization with parvalbumin [Grill et al., 1998b].

METHODS

Double labeling was used to determine the neurochemical identity of neurons which were active during reflex micturition. All animal care and experimental procedures were according to NIH guidelines and were reviewed and approved by the Institutional Animal Care and Use Committee of Case Western Reserve University.

Experimental Preparation

Sexually-intact male cats were anesthetized with xylazine (Rompun, 2.0 mg/kg, SQ) and ketamine HCl (Ketaset, 15 mg/kg, IM), a venous catheter was inserted in the cephalic vein, and anesthesia was maintained with alpha-chloralose (Sigma, 60 mg/kg IV). Animals were intubated, body temperature was maintained with a recirculating water pad, and the electrocardiogram was monitored. The skin around all incision sites was anesthetized with bupivacaine HCl (Marcaine, 0.5%, 1 cc injected ID and SQ) in an effort to reduce surgically induced c-fos expression. A ventral midline incision was made to expose the pre-prostatic urethra rostral to the pubic symphysis. The bladder was cannulated per-urethrally with a polyethylene catheter (o.d. 1 mm), and the catheter was fixed in place with a tie around the pre-prostatic urethra (1/8" wide cotton umbilical tape, 10-A, Ethicon, Somerville, NJ). The incision was closed in layers and the catheter was connected to a pressure transducer in series with a constant flow infusion pump. The pressures generated in the bladder were measured using a solid state pressure transducer connected to the bladder catheter (Deltran DPT-100, Utah Medical Products, Midvale, UT). The pressure signals were amplified, low pass filtered (fc=30 Hz), and recorded on a strip chart recorder.

Stimulation to Induce Expression of c-Fos

A two hour period of isometric micturition induced by bladder filling (1 ml/min with room temperature saline) was used as the stimulus to induce c-fos expression. One to 2 hours after the period of stimulation, the animals were perfused via the aorta with saline followed by 4% paraformaldehyde in 0.1M $NaPO_4$ (pH=7.4). The brain and spinal cord were removed, stored in fixative for 2-5 days, and then transferred to 30% sucrose in 0.1M $NaPO_4$ (PBS) for 2-4 days.

3

Tissue Processing

The sacral spinal cord was sectioned transversely at 50 μm intervals on a freezing microtome and a 1 in 5 series of sections were processed for immunocytochemical detection of Fos protein and GABA. Floating sections were rinsed in phosphate buffered saline (PBS), rinsed in PBS containing 0.3% Triton X-100, and then exposed for 30 min to PBS-Triton solution containing 3% normal rabbit serum to block non-specific binding sites. After a wash in PBS-Triton, the sections were exposed overnight at room temperature in a primary polyclonal antibody solution (rabbit anti-Fos, 1:10,000 in PBS, Calbiochem). After rinsing in PBS, sections were exposed to secondary antibody (biotinylated goat anti-rabbit, Calbiochem) for 1 h and further processed using a standard biotin avidin peroxidase kit (ABC-Elite, Vector Labs, Burlingame, CA). The immunoreaction was visualized by incubating the sections with 0.02% 3.3'-diaminobenzidine containing 0.01% H_2O_2 for 6 minutes. A purple-black reaction product was obtained by adding $NiCl_2$ to the peroxidase reaction (40 μl of 8% $NiCl_2$ solution per 100 ml of DAB solution). Sections were rinsed twice in PBS, washed in PBS-Triton, and then exposed overnight at room temperature in a second primary polyclonal antibody solution (rabbit anti-GABA, 1:200 in PBS-Triton, Chemicon). After rinsing in PBS, sections were exposed to secondary antibody (biotinylated goat anti-rabbit, Calbiochem) for 1 h and further processed using a standard biotin avidin peroxidase kit (ABC-Elite, Vector Labs, Burlingame, CA). The immunoreaction was visualized by incubating the sections with 0.02% 3.3'-diaminobenzidine containing 0.01% H_2O_2 for 6 minutes. The sections were rinsed in PBS, mounted on gelatin-coated glass slides, air dried overnight, cleared in xylene, counter stained with 0.6% thionin in 0.2 M acetic acid buffer (pH 4.5), and coverslipped.

Visualization and Quantification

Stained sections were viewed using bright-field microscopy and the locations of cells exhibiting immunoreactivity described according to the conventions of Rexed for the spinal cord [Rexed, 1954]. The double immunoctyochemical procedure resulted in a purple-black reaction product in the nuclei of neurons exhibiting Fos immnoreactivity and a brown reaction product in the cytoplasm of neurons immunoreactive for GABA. The numbers of cells expressing Fos immunoreactivity, GABA immunoreactivity, or both in each lamina on each side of the spinal cord were counted by a blinded investigator. High resolution, low magnification prints were made of 3 sections from each spinal segment S1, S2, S3) in each animal. The prints were used to mark immunoireactive cells that were identified by examining the same sections under higher magnification.

RESULTS

As we have reported previously [Grill et al., 1998a] neurons expressing c-Fos immunoreactivity were found bilaterally in S1-S3, with the largest number of cells present in S2. Neurons were localized to the lateral portion of the superficial dorsal horn (laminae I and II), the intermediolateral region (lateral laminae V-VII), and around the central canal (lamina X and medial laminae V-VII) (fig. 1). Comparatively fewer GABA-immunoreactive neurons were observed, and these were restricted to the intermediolateral region (lateral laminae V-VII), and around the central canal (lamina X and medial laminae V-VII) (fig. 1). Less than 5% of neurons were immunoreactive for

4

both c-Fos and GABA (fig. 2). Double-labeled neurons were found both around the central canal and within the intermediolateral region (fig. 1).

These results indicate that few GABAergic neurons are active during reflex micturition. This finding is consistent with our previous data co-localizing c-Fos and parvalbumin [Grill et. al, 1998b], a calcium binding protein present in GABAergic CNS neurons.
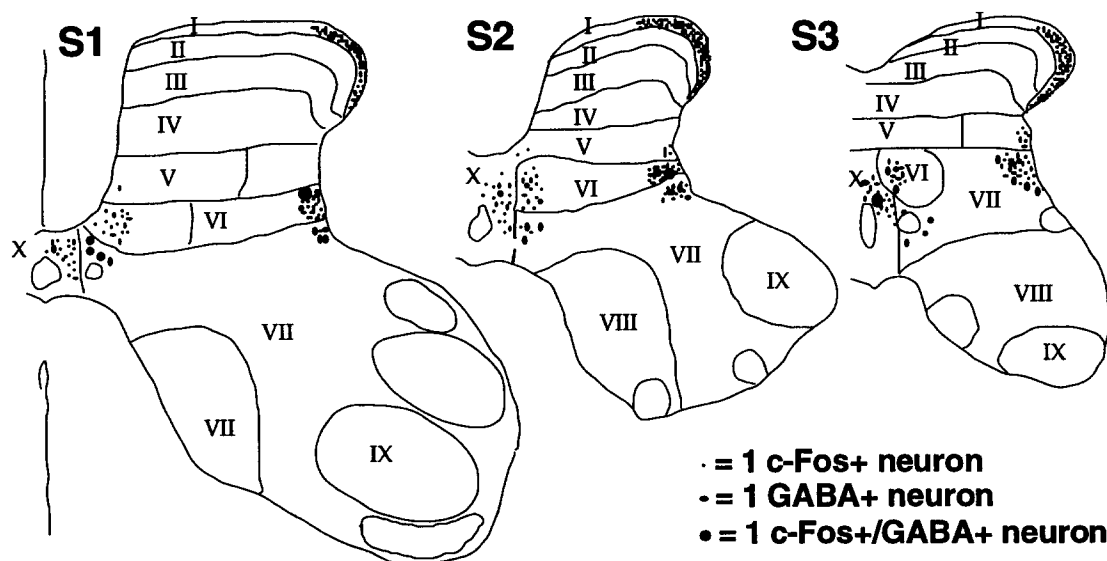

· = 1 c-Fos+ neuron
· = 1 GABA+ neuron
● = 1 c-Fos+/GABA+ neuron

Figure 1: Segmental and laminar distribution of neurons in the cat sacral spinal cord exhibiting c-Fos immunoreactivity, GABA immunoreactivity, or both following a 2 hour period of isometric micturition. Figure shows the mean distribution across 3 sections per segment * 2 animals.
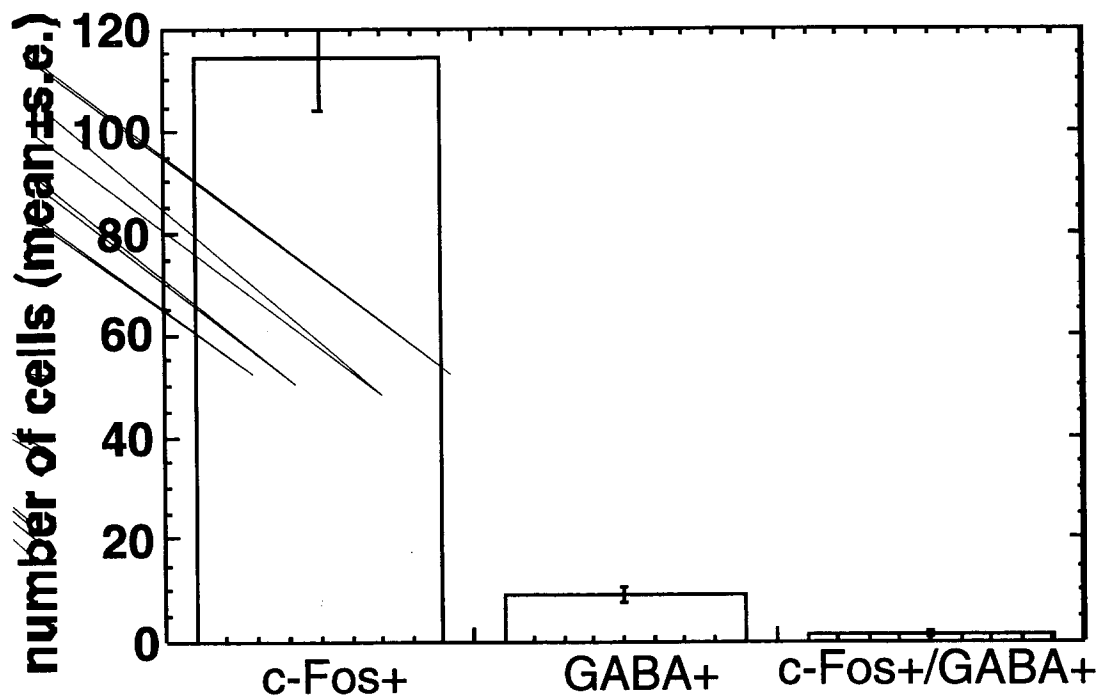
Figure 2: (PREVIOUS PAGE) Number of neurons in the cat sacral spinal cord (S1, S2, S3 combined) exhibiting c-Fos immunoreactivity, GABA immunoreactivity, or both following a 2 hour period of isometric micturition (n=3 sections per segment * 2 animals).

Hindlimb Motor Responses Evoked by Intraspinal Microstimulation

Our previous high-resolution mapping experiments of single joint motor responses identified region of the lumbar spinal cord that produced hindlimb activation. The results demonstrated that maps were repeatable across experiments and that maps of motor responses generated by microstimulation in the ventral horn were in strong agreement with the known location of the motoneurons innervating the knee flexors and extensors. Further, dorsal stimulation produced ipsilateral flexion and contralateral extension- these responses were reminiscent of two classical spinal reflexes- flexion withdrawal and crossed extension.

More recently we have begun a series of experiments to further characterize the hindlimb motor responses evoked by microstimulation. In these experiments rather than recording single joint responses, we are recording the net force at the endpoint of the hindlimb.

METHODS

The endpoint forces evoked at the paw by microstimulation of the lumbar spinal cord were recorded in anesthetized cats. All animal care and experimental procedures were according to NIH guidlines and were approved by the Institutional Animal Care and Use Committee of Case Western Reserve University.

Experimental Preparation

Animals were anesthetized with ketamine HCl (Ketaset, 15-30 mg/kg, IM), a venous catheter was inserted in the cephalic vein, and anesthesia maintained with alpha-chlorolose (Sigma, 60 mg/kg IV, supplemented at 15 mg/kg). A laminectomy was made to expose the lumbosacral spinal cord. The animal was mounted in a frame with pins at the hips, the head in a headholder, and vertebral clamps at L3 and S1. The femur was fixed with a steel pin, and the forces evoked at the paw were recorded using a 3-axis force/moment transducer (Nano-17, ATI Inc., Garner, NC) mounted on an x-y table (fig. 3). Body temperature was maintained between 37° and 39° C with a thermostatically controlled heat lamp, 0.9% saline with 8.4 mg/cc sodium bicarbonate and 5% dextrose added was administered IV (~20 cc/hr), respiration was maintained with a respirator, and electrocardiogram was monitored throughout the experiment. Dexamethasone (2 mg/kg) was administered at the completion of the laminectomy and every 6 hours thereafter for the duration of the experiment.

The dura was opened, the levels identified by root exit, the spinal cord was covered with warm mineral oil, and microstimulation commenced. Vertical, dorsal-to-ventral penetrations were made to position electrodes at locations identified in our previous high-resolution mapping studies to evoke hindlimb motor responses. Activated iridium wire microelectrodes (50 μm diameter) with an exposed electrochemically determined surface area of ~225 μm^2, a 1-3 μm tip, and insulated with Epoxylite were used (IS300, Huntington Medical Research Institutes, Pasadena, CA). Stimuli were charge balanced biphasic pulses with a cathodic phase amplitude of 10-100 μA and

duration of 100 μs applied at 40 Hz for 0.5 s. The amplitude of the anodic phase was limited to 100 μA and the duration was set automatically by the stimulator to balance the charge in the primary phase.
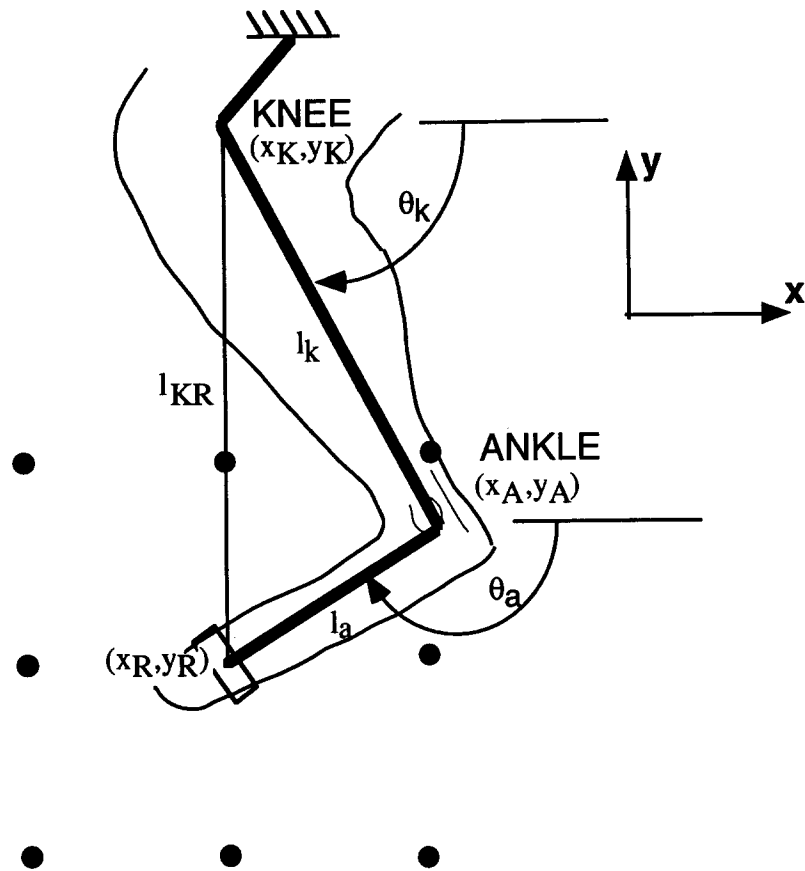

Figure 3: Illustration of the cat hindlimb and the locations in the workspace where the endpoint forces evoked by microstimulation were measured.

For selected electrode positions within the spinal cord, the effect of limb position on the endpoint forces was determined. Forces were recorded at 9-12 different positions of the hindlimb in the workspace. Force signals were amplified, low pass filtered (750 Hz), and sampled by computer. Offline, force signals were low pass filtered at 10 Hz, and the force amplitude quantified by averaging over a 20 ms window centered on the peak force relative to the baseline force averaged over the 1 s interval preceding the stimulus train.

RESULTS

Examples of the endpoint forces evoked by microstimulation at two different depths along a track at the L6/L7 border are shown in fig. 4. The direction of the vector shows the direction of the force, its length is proportional to the force magnitude, and its location on the grid corresponds to the location of the limb endpoint. The nine measurement points are shown by the open cirlces, and to get a more complete picture of the hindlimb response over the workspace, linear interpolation was used to calculate the endpoint force vectors between the measurement points [Giszter et al., 1993]. These data

7

demonstrate that the magnitude and direction of the endpoint force varied as the position of the limb was changed. Recall that the stimulus was the same at each limb location.

The characteristics of the two endpoint force fields are clearly different. The endpoint forces displayed in fig. 4A were evoked by microstimulation at an intermediate depth (3400 μm). The forces were oriented in a flexion direction, and the magnitude and direction of the endpoint forces varied in such a way as to converge to a point in the workspace, shown by the black dot. If the limb were positioned at this location, the data predict that no net endpoint force would be present. Further, the pattern of forces predicts that as the limb is displaced from this point, the muscle forces evoked by microstimulation act to move the limb back to that point. Thus, microstimulation produced a pattern of activation that makes the hindlimb behave as a two dimensional spring.

The endpoint forces displayed in fig. 4B were evoked by microstimulation at a ventral depth (5200 μm) in the region of somatic motor neurons. The force vectors had a parallel or divergent extension pattern, and although the magnitude of the force varied with limb position, the direction was relatively constant.
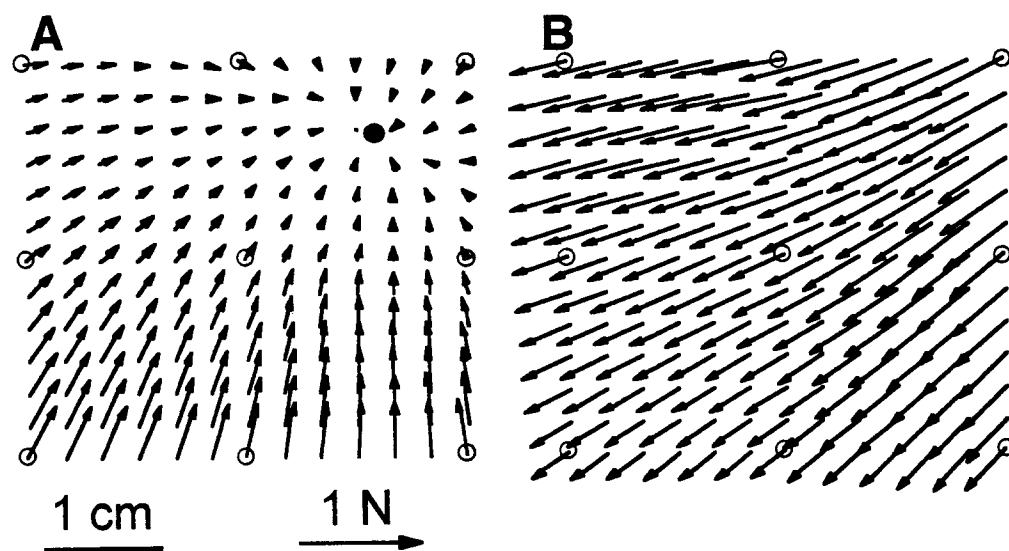

Figure 4: Endpoint forces evoked by microstimulation of the lumbar spinal cord at the L6/L7 border. Each arrow shows the force vector measured at the paw. The length of the vector is proportional to the magnitude of the force, its direction indicates the direction of the force, and its location indicates the location of the hindlimb in the workspace where that force was measured. The open circles are the locations where evoked forces were measured. **A.** Forces evoked by microstimulation in the intermediate region (depth=3400 μm) using a 0.5 s 40 Hz train of 100 μA 100 μs pulses. **B.** Forces evoked by microstimulation in the ventral region (depth=5200 μm) using a 0.5 s 40 Hz train of 15 μA 100 μs pulses.

The previously described data were the patterns of endpoint forces evoked at two locations of microstimulation. The data in fig. 5 show the endpoint forces evoked as a function of the depth of the microelectrode. Again the vector direction is the direction of

the force, and the length of the vectors is proportional to the force magnitude. The important point to notice is that the vector orientation is constant over changes in electrode depth of at least 400 μm. Thus, the neuronal elements producing these responses have some finite spatial extent.
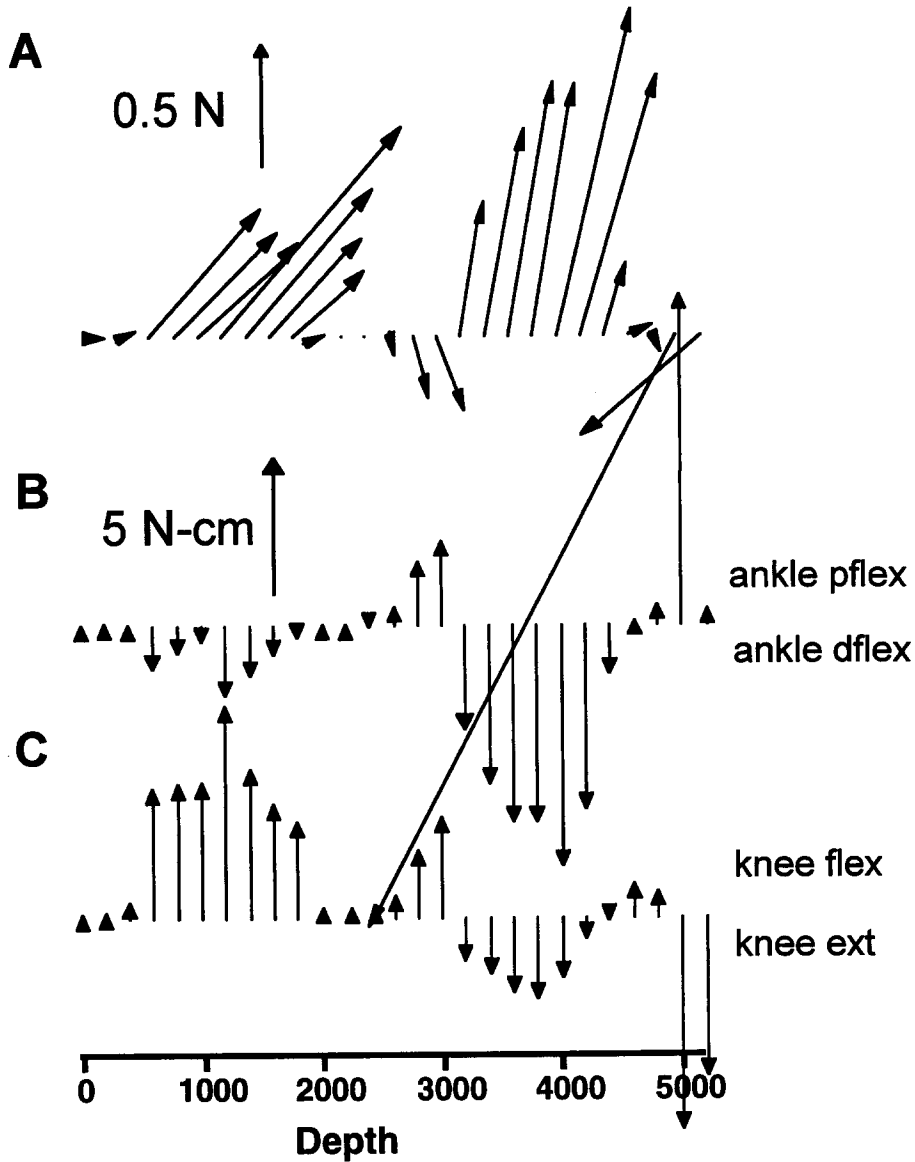

Figure 5: Endpoint force vectors (A), and ankle (B) and knee (C) joint torques evoked by intraspinal microstimulation as a function of depth of the stimulating electrode along a track at the L6/L7 border. Stimulus was a 0.5 s 40 Hz train of 100 μA 100 μs pulses.

Also shown are the torques at the knee and ankle as a function of depth. The individual joint torques were calculated from the limb geometry and the measured endpoint forces (see fig. 3) using the relation T=J^{t}F, where F is a vector of the endpoint forces and J^t is the transpose of the Jacobian given by

$$J'=\begin{bmatrix} -l_k\sin\theta_k -l_a\sin\theta_a & l_k\sin+l_a\sin\theta_a \\ -l_a\sin\theta_a & -l_a\cos\theta_a \end{bmatrix}$$

where l_k and l_a are the lower leg and paw lengths, respectively, and θ_k and θ_a are the knee and ankle joint angles (see fig. 3).

The length of each arrow is proportional to the magnitude of the joint torque and its direction indicates either flexion or extension. The joint torques correspond well to the evoked forces. For example in the region in which the limb is moving up towards the hindquarters ($\sim$1000 μm), the knee torque is in flexion and the ankle is in dorsiflexion.

These results demonstrate that endpoint forces provide a more complete characterization of the hindlimb motor response evoked by microstimulation than did single joint responses. Microstimulation in interneuronal regions produced endpoint forces that converged to a point in the limb workspace. The orientation of the endpoint force vector was preserved over depths of at least 400 μm and the contributions of the ankle and knee varied at different locations in the limb workspace and at different points of microstimulation. In contrast to the results obtained by microstimulation at intermediate depths, microstimulation in the motoneuronal region produced parallel or divergent force fields at the endpoint.

OBJECTIVES FOR THE NEXT QUARTER

In the next quarter we will continue our co-localization studies to identify inhibitory spinal neurons active during micturition. Our specific objectives are to conduct control experiments to examine interactions between the c-Fos reaction product and detection of amino acid neurotransmitters [Todd et al., 1994], and to begin studies co-localizing c-Fos with glycine. We will also continue our studies characterizing the hindlimb motor responses to lumbar microstimulation. Our specific objectives are to determine whether the finding of convergent endpoint force vectors is consistent and to examine a relationship between the location of stimulation and the structure of the endpoint force vectors.

LITERATURE CITED

Giszter, S.F., F.A. Mussa-Ivaldi, E. Bizzi (1993) Convergent force fields organized in the frog's spinal cord. J. Neuroscience 13:467-491.

Grill, W.M., B. Wang, S. Hadziefendic, M.A. Haxhiu (1998a) Identification of the spinal neural network involved in coordination of micturition in the male cat. Brain Research 796:150-160.

Grill, W.M., S. Hadziefendic, B.O. Erokwu, M.A. Haxhiu (1998b) Co-localization of parvalbumin and c-fos in sacral spinal neurons involved in regulation of micturition. Society for Neuroscience Abstracts 24:1618.

Rexed, B. (1954) A cytoarchitectonic atlas of the spinal cord in the cat. J. Comp. Neurol. 100:297-351.

Todd, A.J., R.C. Spike, A.R. Bridbelt, R.F. Price, S.A.S. Shebab (1994) Some inhibitory neurons in the spinal cord develop c-fos-immunoreactivity after noxious stimulation. Neuroscience 63:805-816.